Research article

Shaohua Dong, Qing Zhang*, Guangtao Cao, Jincheng Ni, Ting Shi, Shiqing Li, Jingwen Duan, Jiafu Wang, Ying Li*, Shulin Sun, Lei Zhou, Guangwei Hu and Cheng-Wei Qiu*

On-chip trans-dimensional plasmonic router

https://doi.org/10.1515/nanoph-2020-0078
Received January 31, 2020; accepted March 30, 2020;
published online April 23, 2020

Abstract: Plasmons, as emerging optical diffraction-unlimited information carriers, promise the high-capacity, high-speed, and integrated photonic chips. The on-chip precise manipulations of plasmon in an arbitrary platform, whether two-dimensional (2D) or one-dimensional (1D), appears demanding but non-trivial. Here, we proposed a meta-wall, consisting of specifically designed meta-atoms, that allows the high-efficiency transformation of propagating plasmon polaritons from 2D platforms to 1D plasmonic waveguides, forming the trans-dimensional plasmonic routers. The mechanism to compensate the momentum transformation in the router can be traced via a local dynamic phase gradient of the meta-atom and reciprocal lattice vector. To demonstrate such a scheme, a directional router based on phase-gradient meta-wall is designed to couple 2D SPP to a 1D plasmonic waveguide, while a unidirectional router based on grating metawall is designed to route 2D SPP to the arbitrarily desired direction along the 1D plasmonic waveguide by changing the incident angle of 2D SPP. The on-chip routers of trans-dimensional SPP demonstrated here provide a flexible tool to manipulate propagation of surface plasmon polaritons (SPPs) and may pave the way for designing integrated plasmonic network and devices.

Keywords: metasurface; plasmonic circuit; plasmon propagation; router; surface plasmon.

Shaohua Dong and Qing Zhang: These authors contributed equally to this work.

***Corresponding authors: Cheng-Wei Qiu and Qing Zhang**, Department of Electrical and Computer Engineering, National University of Singapore, Kent Ridge, Singapore, 117583, Singapore, E-mail: chengwei.qiu@nus.edu.sg; elezqing@nus.edu.sg; **Ying Li:** SZU–NUS Collaborative Innovation Center for Optoelectronic Science & Technology, International Collaborative Laboratory of 2D Materials for Optoelectronics Science and Technology of Ministry of Education, Institute of Microscale Optoelectronics, Shenzhen University, Shenzhen, 518060, PR China, E-mail: queenly@vip.sina.com. https://orcid.org/0000-0002-5989-1229 (Q. Zhang)
Shaohua Dong: SZU–NUS Collaborative Innovation Center for Optoelectronic Science & Technology, International Collaborative Laboratory of 2D Materials for Optoelectronics Science and Technology of Ministry of Education, Institute of Microscale Optoelectronics, Shenzhen University, Shenzhen, 518060, China; Department of Electrical and Computer Engineering, National University of Singapore, Kent Ridge, Singapore, 117583, Singapore
Guangtao Cao, Jincheng Ni, Ting Shi and Guangwei Hu: Department of Electrical and Computer Engineering, National University of Singapore, Kent Ridge, Singapore, 117583, Singapore
Shiqing Li, Jingwen Duan and Shulin Sun: Shanghai Engineering Research Center of Ultra-Precision Optical Manufacturing, Green Photonics and Department of Optical Science and Engineering, Fudan University, Shanghai, 200433, PR China. https://orcid.org/0000-0003-3046-1142 (S. Sun)
Jiafu Wang: Department of Basic Sciences, Airforce Engineering University, Xian, 710051, PR China
Lei Zhou: State Key Laboratory of Surface Physics and Key Laboratory of Micro and Nano Photonic Structures (Ministry of Education), Fudan University, Shanghai, 200433, PR China

1 Introduction

Surface plasmon polaritons (SPPs) have been viewed as an emerging candidate of information technologies, thanks to its diffraction-unlimited profile, strong evanescent confinement (i. e., the small skin depth), convenient readout with electronic signals, the high-speed operation, the high-capacity storage, and others [1, 2]. Thus, the arbitrary manipulation of their propagation is of fundamental importance to develop the next-generation plasmonic networks and circuits that are assembled in a chip. For a classification of plasmonic devices based on the dimensional propagation, 2D plasmonic devices allow the wave propagations at any in-plane directions such as the SPP on a dielectric/metal surface excited by a point source, while 1D devices, essentially like a strip waveguide, could only support the SPP propagation in a fixed distinguished direction. The past decade has witnessed the development of control of 2D SPPs at the dielectric/metal interface, which offer many applications in practice, such as focusing [3–8], demultiplexer [9], Airy-beam generation [10, 11], cloaking [12, 15], hyperbolic propagation[13, 14], and so on. For 1D plasmonic system, it has offered extensive applications in plasmonic circuits, such as logic gates [16, 17], router in nanowire networks [18,

19], SPP mode decoupling [20], plasmonic SPP waveguides [21–26], Y-splitters [27], and so on. The exciting achievement to manipulate SPPs in different geometric dimensions (2D and 1D) has shown the conceivable potentials of plasmonic devices for the information technologies, but a missing gap lies in the flexible transformation and compatibilities between these two kinds of devices.

Meta-surfaces, consisting of arrays of artificially designed sub-wavelength compositions, provide a powerful tool to control electromagnetic waves. By accurately engineering its sub-wavelength inclusions to modulate the local wavefront, many fascinating phenomena and applications have been demonstrated, including anomalous refraction/reflection [28, 29], giant photonic spin hall effect [30–32], holograms [33–36], metalens [37–39], surface plasmon excitations [40–42], and so on. However, unlike arbitrarily controlling of propagating waves in free space, direct manipulation of the evanescent SPP is hard, especially when the high efficiency is involved, because of the important radiative scattering channel to free space. Recently, we extend the concept of the metasurface to build high-efficiency metawall in reflection geometry for arbitrary SPP engineering which demonstrated an anomalous reflection, SPP metalens and Bessel beam generation [6, 7]. However, it remains elusive and largely unknown how a transmissive control of SPP could be achieved along with the multifunctional and high-efficiency operation in high frequencies.

In this work, we propose transmission-type meta-walls at a telecommunication wavelength (i. e.,1550 nm), which are constructed simply by the standing dielectric slabs. The width of the slabs can be tuned to program the phase of transmitted SPP while the magnitude of the transmission remains large, thus to allow the anomalous deflection and focusing of SPPs in a close analog of the achievable of electromagnetic meta-surface in free space [28]. More importantly, to bridge the link between 2D and 1D plasmonic systems, an on-chip trans-dimensional router is first demonstrated to directly transform a 2D SPP beam to the SPP in 1D plasmonic waveguide with a drastic momentum change of 90 degrees, whose remarkable momentum mismatch are compensated by the linear phase gradient provided by the meta-wall. Further, we realize the unidirectional SPP routers based on grating metawall scheme which provides the reciprocal lattice vector to compensate the momentum mismatch between the two types of plasmonic systems. By changing the incident angle of 2D SPP, we can efficiently route the 2D SPP beams to the desired directions along the plasmonic waveguide. Our results open a new avenue of designing cross-platform photonic devices.

2 Results

We start by introducing the concept of on-chip router of trans-dimensional plasmons. For simplification, we suppose a simple on-chip plasmonic system composed of a flat metal surface and a dielectric waveguide placed on it, as schematically shown in Figure 1A. The flat plasmonic metal can support a 2D SPP eigenmode (with the wavevector of k_{2DSPP}) along x direction, while the plasmonic waveguide can support a 1D SPP mode (with the wavevector of k_{1DSPP}) propagating along y direction. The orthogonally of two

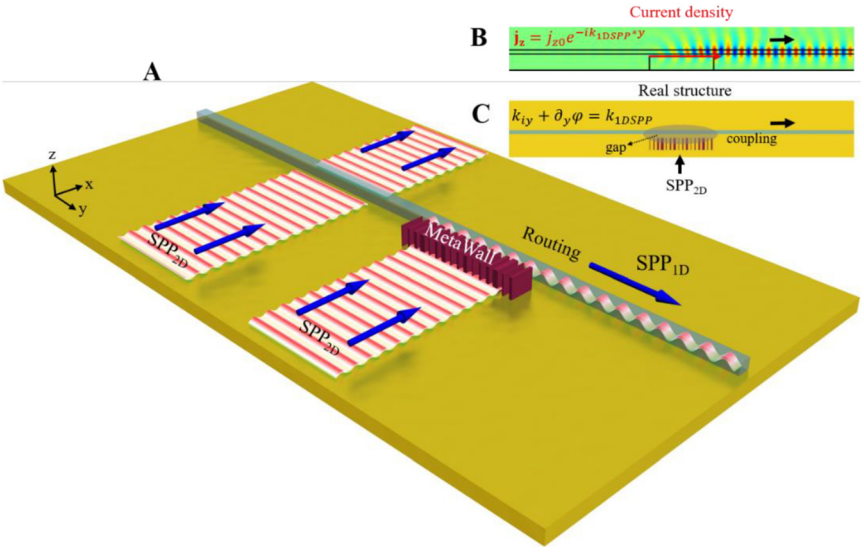

Figure 1: The schematic of on-chip SPP router for coupling an inputting 2D SPP beam to a 1D plasmonic waveguide. (A) Schematic of the SPP router based on metawall constructed by arrays of standing dielectric slabs with different thicknesses on metal base. A 2D SPP beam can be routed to the vertical direction along the plasmonic waveguide when a meta-wall placed near the plasmonic waveguide compared with nothing here (B) A current element model ($j_z = j_{z0}e^{-ik_{1DSPP}*y}$) built to demonstrate a 1D SPP mode can be excited in the plasmonic waveguide by the designed 2D surface current density distribution with the phase-gradient along y equal to the eigenvector k_{1DSPP} of the 1D SPP mode. Where j_{z0} is amplitude distributes along z direction of the SPP eigenmode on the metal base. (C) A real model based on meta-wall designed to mimic the current element model. The transmission field distribution of the meta-wall can be equivalent to j_z for a 2D SPP beam striking on the meta-wall.

wave vectors in the system implies a very large momentum mismatch so that the information loaded by the propagating 2D SPPs is difficult to be delivered to the plasmonic waveguide (see the left case in Figure 1A). This scenario is in a close analog of converting 3D free space wave into 2D near-field SPP [40, 42], except the fact that what we aimed to achieve is the steering or transformation of plasmonic near fields. Here, we realize an arbitrary phase distribution of SPP, such as a linear gradient phase for the compensation of plasmonic momentum mismatch from 2D to 1D plasmonic system, so that the impinging 2D SPP can be efficiently routed into the 1D plasmonic waveguide (see the right case in Figure 1A). To demonstrate the feasibility, we first build a 2D current element model to mimic the momentum match. A 2D surface current source with the current density distribution of $j_z = j_{z0}e^{-ik_{1D,SPP}*y}$ is placed at an appropriate distance from the plasmonic waveguide to excite the 1D SPP mode in the plasmonic waveguide, where j_{z0} is the amplitude distribution along z direction of the 2D SPP eigenmode in the plasmonic metal. As shown in Figure 1B, the 1D SPP mode in the plasmonic waveguide is well excited by a 2D current element model as expected, of which the specific details will be present later. To realize the 2D current element model by the practical structure, we propose the phase-gradient metawall constructed by arrays of standing dielectric slab on a plasmonic metal, as shown in Figure 1C. When a 2D SPP strikes the meta-wall, the local transmission phase of each meta-atom need to be the same with the corresponding current element at same position so that the transmission-phase distribution satisfying $k_{iy} + \partial_y\varphi = k_{1DSPP}$, where k_{iy} is the y-component of k_{2DSPP}, φ is local transmission-phase of meta-atom and $\partial_y\varphi$ is the phase gradient along y directions. Fundamentally, the momentum match determines whether the modes can be routed from one system to another, while there is another important factor that the coupling intensity between two modes will decide how much energy can be routed from one system to another. Therefore, except the momentum match problem, the coupling intensity should also be considered together to improve the meta-wall performance.

We now introduce how to build a meta-wall to realize the arbitrary phase distribution. Obviously, the key is to find a kind of meta-atom architecture with high efficiency in transmission geometry. We design a single-layer metastructure constructed by a TiO_2 dielectric slab with adjustable thickness to satisfy the requirement at the wavelength of 1550 nm. Figure 2A shows the simulation setup where the SPP transmission coefficient can be obtained for a non-gradient meta-wall consisting of arrays of TiO_2 dielectric slab (length d = 1.4 μm) standing on an Au film with periodicity a = 400 nm along y direction. Here, the SiO_2 slab placed on the Au film has a thickness of 100 nm, thus to allow the eigenmode of 2D SPP more localized ($k_{2DSPP} = 1.0509k_0$). Considering the radiation losses to the far field, the vertical height of the meta-wall does not need to be very large but should be necessarily larger than the decay length (about 382 nm) of the 2D SPP, which is set as 1 μm here. The refractive indexes of TiO_2 and SiO_2 are set as 2.4328 and 1.45 at 1550 nm respectively [43]. Based on the same configuration, Finite element method (FEM) is utilized to simulate the S-parameter, the transmission amplitude and phase of SPP as shown in Figure 2B. Figure 2B shows that the phase of transmitted SPP can cover the full range of 2π with the thickness (w) varying from 40 to 340 nm at the working wavelength of 1550 nm. Meanwhile, the transmission amplitude can also keep a high value (larger than 0.81) in the whole spectrum. To preliminarily demonstrate the performance of the meta-atom, we build a phase-gradient meta-wall constructed by the super cell consisting of 6 sub-units (w = 50, 81, 120, 167, 224, and 290 nm) that satisfies the transmission phase distribution $\varphi(y) = \varphi_0 + \xi y$, where the phase gradient $\xi = 0.62k_{2DSPP}$. Based on the momentum conservation along y direction, the transmitted SPP need to satisfy:

$$k_{iy} + \xi = k_{ty} \tag{1}$$

where $k_{iy} = k_{2DSPP}\sin\theta_i$ is the y-component of k_{2DSPP}, ξ is the phase gradient provided by the metawall, and $k_{ty} = k_{2DSPP}\sin\theta_t$ is the y-component of wave vector for the transmission SPP, θ_i and θ_t are the incident and transmission angles of respectively. According to Eq. (1), the transmission angle of SPP is predicted as 38° at the normal incidence. We use Finite element method (FEM) simulations to calculate the near-field E_z pattern when a Gaussian SPP beam is launched to strike normally on the meta-wall. As shown in Figure 2C, the SPP beam through the meta-wall does flow along the direction, indicating an excellent agreement with the theoretical expectation. Through the energy flow integral, the anomalous transmission efficiency can be evaluated as about 70%. Moreover, a more complex wave front manipulation of SPP focusing effect is further demonstrated (see Figure 1S of Supplementary Materials), which also shows a favorable performance.

Then, we demonstrate a directional SPP router based on meta-wall to establish a relationship between 2D SPP and 1D SPP systems. Here, a SiO_2 dielectric waveguide with cross section area of 400 × 400 nm^2 is placed on top of the plasmonic metal, which supports a 1D hybrid SPP mode with the wavevector of $k_{1DSPP} = 1.1527k_0$ (see Figure S2A of Supplementary Materials). In this case, the SPP trans-

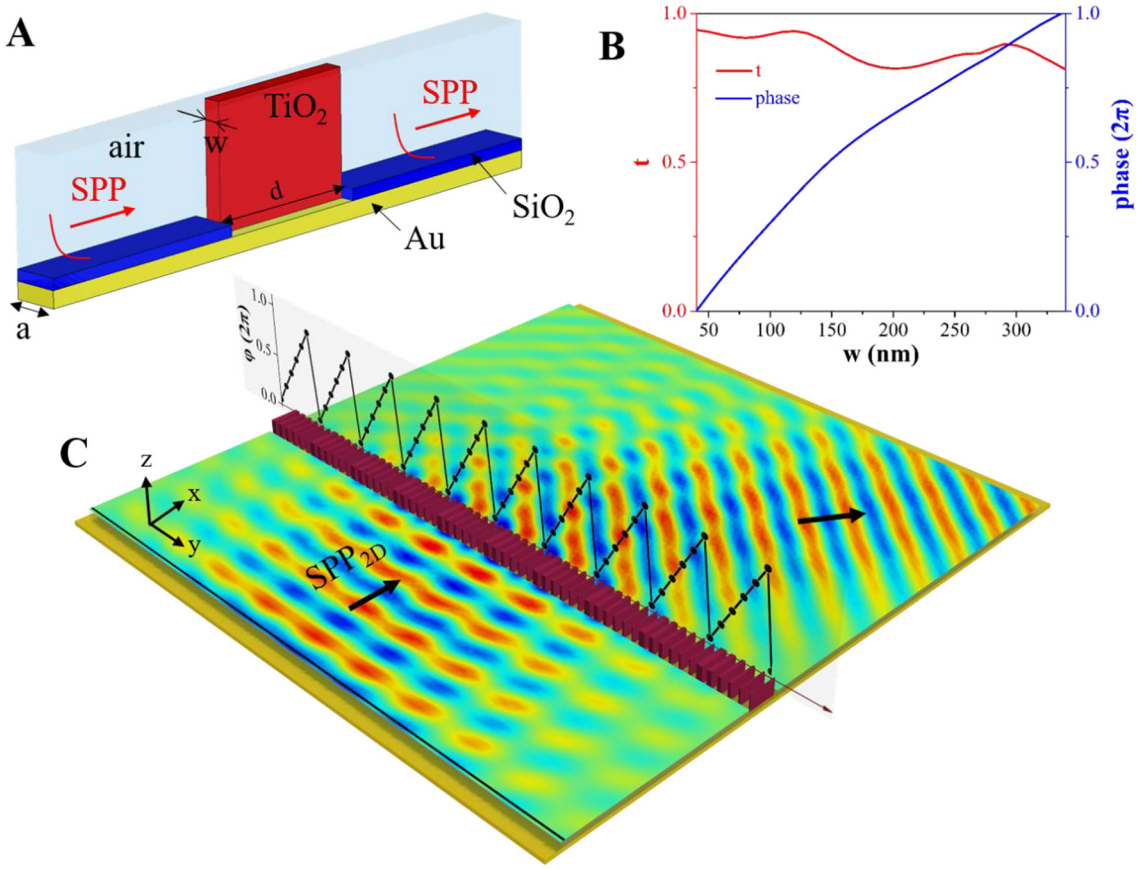

Figure 2: Unit cell design and demonstration of meta-wall. (A) Simulation setup to obtain the SPP transmission coefficient of a non-gradient meta-wall composed of a TiO_2 slab (d = 1.4 μm, a = 400 nm). By changing the width w of the meta-wall, the transmission phase of SPP can be modulated freely. (B) FEM-simulated transmission amplitude and phase of SPP versus the width w. (C) FEM-simulated near-field E_z pattern on a plane above the plasmonic metal for a SPP Gaussian beam striking the meta-wall at normal incidence. Here, the w distribution of the meta-wall is designed to satisfy a phase gradient $\xi = 0.62k_{2DSPP}$.

dimensional router can be characterized by the coupling efficiency, representing the amount of incident power being coupled to the plasmonic waveguide along the expected direction (e. g., $+y$ direction in this case), and the directivity D, describing the ratio of SPP power routed in plasmonic waveguide along the expected positive direction (e. g., $+y$ direction) and the opposite direction (e. g., $-y$ direction). Based on the previous analysis, the basis condition of routing 2D SPP to 1D plasmonic waveguide is the momentum match (i. e., $k_{ty} = k_{1DSPP}$). According to Eq. (1), the phase-gradient $\xi = k_{1DSPP}$ provided by the meta-wall is larger than k_{2DSPP} at normal incidence in this case, which will lead to the evanescent transmission field of meta-wall along x direction, meaning the transmission field is not a steady propagating eigenmode on the metal surface but a transient evanescent field. As a result, a suitable width of gap between the meta-wall and the plasmonic waveguide is need for the sake of obtaining the higher coupling efficiency of the evanescent field with the 1D SPP modes in the plasmonic waveguide. Considering the decoupling effect (i. e., the SPP propagating in the waveguide can also couple out by the meta-wall), the router based on meta-wall should not be too wide, so only 16 sub-units are chosen here. Based on this configuration, we use FEM simulations to calculate the coupling efficiency and directivity of the router versus the width w_{gap} of gap. As shown in Figure 3A, we can see that he coupling efficiency can reach a maximum of 29% and the corresponding directivity D is equal to 37 as w_{gap} = 210 nm. Figure 3B shows the near-field E_z pattern for a Gaussian SPP beam launched to strike the meta-wall at normal incidence. Obviously, we can see that the impinging 2D SPP beam is directionally routed to the expected $+y$ direction along the plasmonic waveguide while the 1D SPP propagating along the opposite direction is greatly suppressed. It is noted that the reciprocal lattice vector introduced by the supercell (i. e., with imperfect gradient-phase distribution) will also affect the directional routing performance, besides the imperfect transmission

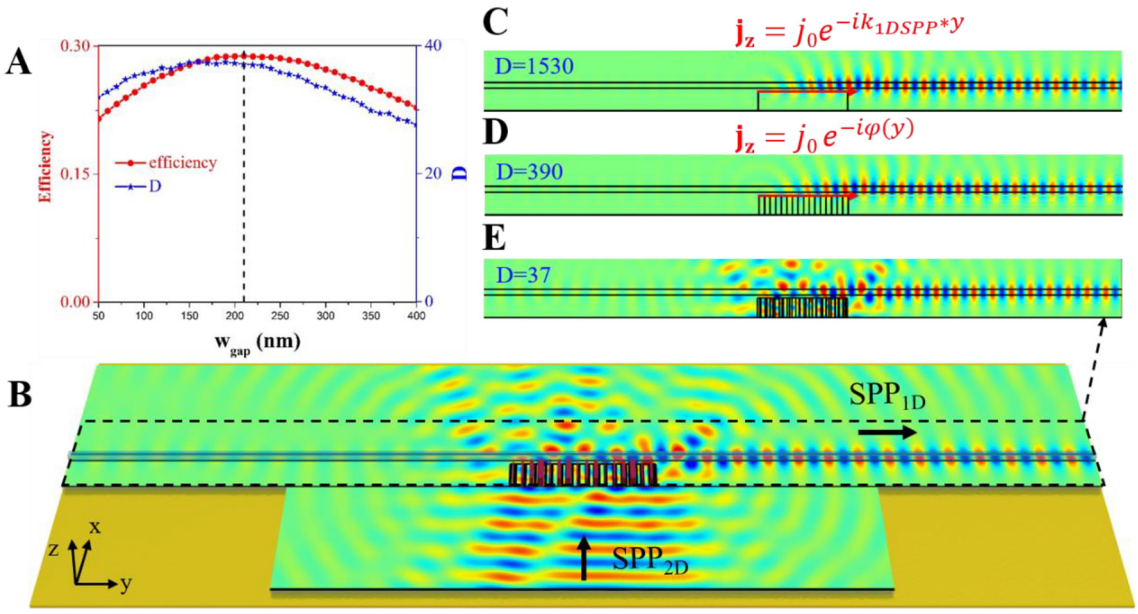

Figure 3: Demonstration of the directional router of trans-dimensional SPP based on phase-gradient meta-wall. (A) The directional coupling efficiency and directivity of the SPP router versus the width w_{gap} of gap between the meta-wall and the plasmonic waveguide (B) FEM-simulated near-field E_z pattern on a plane above the plasmonic metal for a SPP Gaussian beam striking the meta-wall with the phase gradient $\xi = k_{1DSPP}$. The 1D SPP eigenmode of the plasmonic waveguide can be excited under the cases of the continuous current element model (C), the discrete current element model (D) and the meta-wall based on real structure (E).

meta-atoms of meta-wall. Therefore, there are still quite some energy unutilized, where the missing powers are carried out by the scatterings to the far field (about 20%), 0-order transmission of SPP (about 44%), normal reflection (about 1%), in the case of w_{gap} = 210 nm. In order to approach the ideal case, we build the current element model to mimic the ideal trans-dimensional router of SPPs. Figure 3C shows the near-field pattern for a continuous current element model with the current density distribution $\mathbf{j_z} = j_{z0}e^{-ik_{1DSPP}*y}$ placed in the same distance from the plasmonic waveguide with the meta-wall, which demonstrate a much better directivity of D = 1530 than the meta-wall. When we place a discrete current element distribution with the same phase distribution $\varphi(y)$ with the meta-wall, the routing directivity can reach 390, as shown in Figure 3D. For a comparison with the current element models, the near-field pattern in the same region for the proposed router based on meta-wall is shown in Figure 3E. Comparing the continuous one, the discrete current element model with imperfect gradient-phase distribution possesses a smaller directivity, which has larger directivity compared with the real structure due to the imperfect transmission meta-atoms where the disturbances to local phases of meta-wall originating from the coupling among meta-atoms and between waveguide and meta-atoms also cannot be neglected. These theoretical results imply the router based on meta-wall could be further improved, e. g., global optimization to the super cell of meta-wall, while our aim here is to demonstrate the great potentials of meta-wall in trans-dimensional router.

Further, we introduce another scheme that the reciprocal lattice vector provided by a grating meta-wall can be exploited to compensate the momentum mismatch, leading to a unidirectional SPP router depending on the incident angle variation. Similar with Eq. (1), the momentum conservation in this case can be described as:

$$k_{iy} + mK = \pm k_{1DSPP} \tag{2}$$

where $K = 2\pi/\Lambda$ is the reciprocal lattice vector induced by the periodicity of grating meta-wall, Λ is the period of grating meta-wall and m (±1, ±2, …) denotes the order of the diffraction channels of SPP. Here, m just takes ±1 order to match the SPP mode in the waveguide while ignoring higher modes with less influence to the system. For the simplest case of $K = k_{1DSPP}$ for a normal incidence of SPP (i. e., k_{iy} = 0), both of ±1 orders could be routed into the plasmonic waveguide along $+y$ and $-y$ direction respectively. For the new architecture, the number of periods, the thickness (d) and the width (w) of the TiO_2

dielectric slab need to be fixed besides w_{gap}. For simplifying model, 50% duty ratio (i. e., $w = \Lambda/2$) and 11 periods for the TiO_2 dielectric slab is chosen in the design of grating meta-walls. Through optimizing d and w_{gap} to achieve a better coupling efficiency, we get d = 620 nm and w_{gap} = 370 nm here (see Figure S2 of Supplementary Materials). Then, a trans-dimensional SPP router with bidirectional channel is designed. When $k_{iy} \neq 0$ (i. e., $\theta_i > 0$ or $\theta_i < 0$), here we just need analyze the case of $\theta_i > 0$ because responses of the SPP router should be parity symmetric in the cases of $\theta_i < 0$ and $\theta_i > 0$, as determined by the symmetry of this router geometry. For the case of $k_{iy} \neq 0$, we keep the same geometry parameters of grating meta-wall with the ones used in previous case of normal incidence except the value of Λ. Considering $k_{1DSPP} > k_{iy}$, there are only two solutions for Eq. (2), which corresponding to $k_{2DSPP} \sin\theta - K = -k_{1DSPP}$ and $k_{2DSPP} \sin\theta + K = k_{1DSPP}$. For the solution of $k_{2DSPP} \sin\theta - K = -k_{1DSPP}$, Figure 4A shows the vector relationship of momentum match. Obviously, the −1-order mode ($m = -1$) satisfies momentum match with the 1D SPP mode of the plasmonic waveguide and thus should be efficiently routed to −y direction along the plasmonic waveguide, while the +1-order mode ($m = +1$) should be less routed to +y direction along the plasmonic waveguide due to the fact that its wave vector is larger than the required k_{1DSPP} and the propagating wave vector k_{2DSPP} of 2D SPP. For example, supposing the incident angle θ_i = 10°, Figure 4B shows FEM-simulated scattering near-field E_z pattern, which demonstrates that an oblique SPP Gaussian

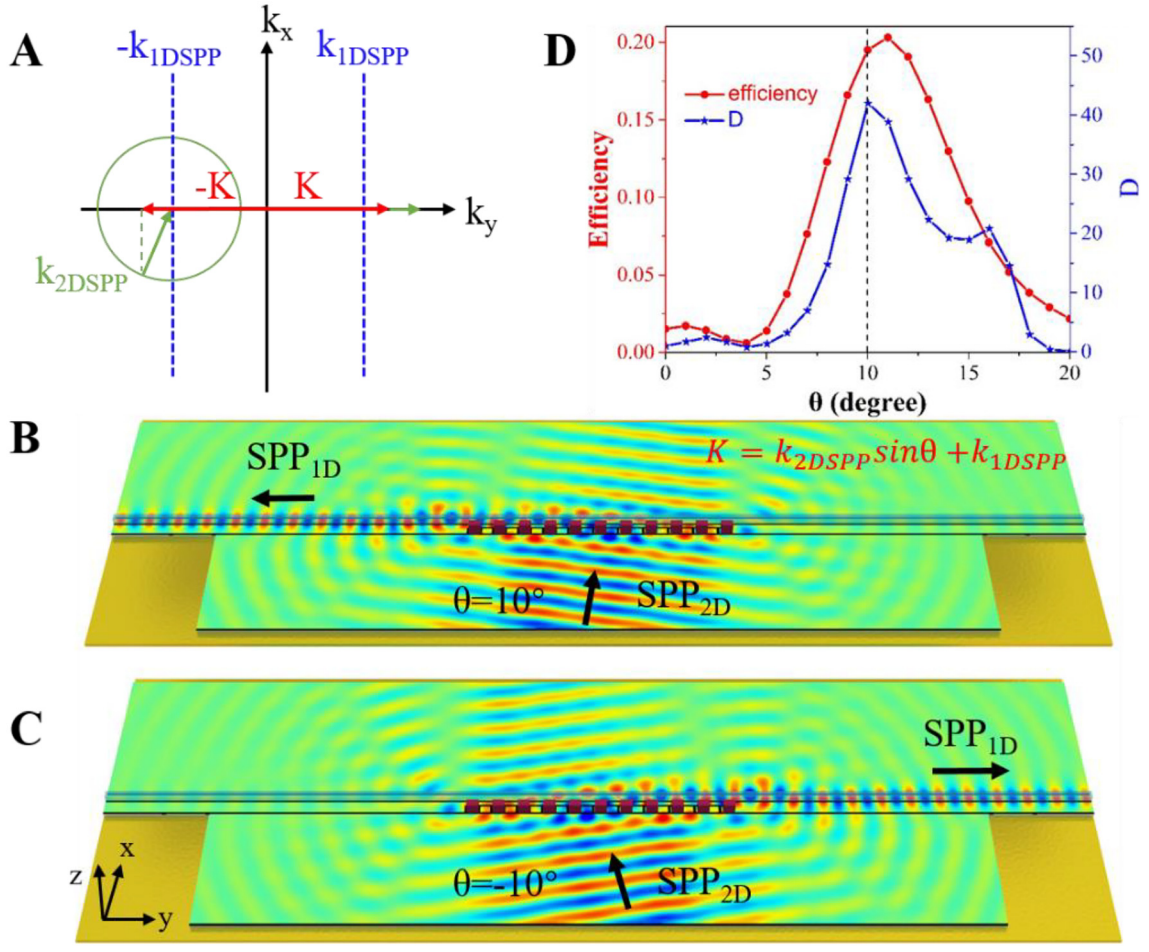

Figure 4: Demonstration of an undirectional SPP router based on the grating meta-wall. (A) Schematic of the momentum mismatches between the inputting 2D SPP and the 1D SPP along the plasmonic waveguide compensated by the reciprocal lattice vector of the grating meta-wall. FEM-simulated near-field E_z pattern on a plane above the plasmonic metal for a SPP Gaussian beam striking the grating meta-wall for the incident angle θ = 10° (B) and θ = −10° (C) respectively under the case of the designed reciprocal lattice vector satisfying $K = k_{2DSPP} \sin\theta + k_{1DSPP}$ (D) The coupling efficiency and directivity of this unidirectional SPP router versus the incident angle θ of 2D SPP.

beam is indeed routed to $-y$ direction along the plasmonic waveguide, while the SPP mode along $+y$ direction does not appear. Moreover, we show the response at the incident angle $\theta_i = -10°$ in Figure 4C, which agrees very well with the previous analysis. To further test the robustness of momentum mismatch in the router based on grating meta-wall, we calculate the coupling efficiency and directivity of the router versus the incident angle by FEM simulations, as displayed in Figure 4D. The coupling efficiency around the designed angle of incidence reaches a maximum (i. e., 20.3% at $\theta_i = 11°$) and the directivity also reaches the maximum of 42 at the designed $\theta_i = 10°$. Such results show that the router is robust with the incidence angle varying from 8° to 17° where the directivity bigger than 10. Around $\theta_i = 2°$ and $\theta_i = 16°$, two other local maximum values appear, which reflects that the routing efficiency cannot be uniquely determined by the momentum match. Because the structure parameters of grating meta-wall in this case are optimized under the condition of $\theta_i = 0°$ rather than $\theta_i°\neq°0°$, the variation of θ_i not only changes the incident momentum k_{iy} but also disturbs the coupling intensity of the two systems, which may lead to multiple extremums. Furthermore, it is noted that the routing performance shown in Figure 4D are achieved under the conditions of $w = \Lambda/2$ and $\theta_i = 0°$, meaning that the unidirectional router could be further improved for other specific cases. For the case of $k_{2DSPP} \sin\theta + K = k_{1DSPP}$, the similar demonstrations can be shown (see Figure S3 of Supplementary Materials). Interestingly, the router based on this configuration can obtain an excellent directivity of 326 at $\theta_i = 7°$, although the efficiency is lower than the previous case of grating meta-wall.

3 Conclusions

To summarize, we extend the concept of free-space meta-surface to build on-chip meta-devices for plasmonic manipulation. The proposed meta-wall consists of arrays of TiO_2 dielectric slab standing on a plasmonic metal in transmission geometry, which can realize arbitrary wave front control of SPP with high efficiency. As the proof of concept, the SPP routers of trans-dimension from 2D to 1D plasmonic system are demonstrated at the wavelength of 1550 nm. For compensating the momentum mismatch of SPPs from 2D to 1D plasmonic system, a scheme based on phase-gradient meta-wall leads to the directional SPP router which just allows the 2D SPP routed to the fixed direction along the 1D plasmonic waveguide, while another scheme based on grating meta-wall leads to the unidirectional SPP router which can route the 2D SPP to the arbitrarily designed direction along the 1D plasmonic waveguide through adjusting the incident angle of SPP. Our findings improve the compatibility of cross-dimensional platform for plasmonic system and may inspire many new on-chip photonic devices.

Acknowledgments: This work was supported by A*STAR Pharos Program (grant number 15270 00014, with project number R-263-000-B91-305), the National Research Foundation, Prime Minister's Office, Singapore, under its Competitive Research Program (CRP award number NRFCRP 15-2015-03), and the National Natural Science Foundation of China (grant no. 61865006 and 11564014).

References

[1] W. L. Barnes, A. Dereux, and T. W. Ebbesen, "Surface plasmon subwavelength optics," *Nature*, vol. 424, no. 6950, pp. 824–830, 2003, https://doi.org/10.1038/nature01937.

[2] R. Zia, J. A. Schuller, A. Chandran, and M. L. Brongersma, "Plasmonics: the next chip-scale technology," *Mater. Today*, vol. 9, no. 7–8, pp. 20–27, 2006, https://doi.org/10.1016/S1369-7021(06)71572-3.

[3] L. Feng, K. A. Tetz, B. Slutsky, V. Lomakin, and Y. Fainman, "Fourier plasmonics: diffractive focusing of in-plane surface plasmon polariton waves," *Appl. Phys. Lett.*, vol. 91, no. 8, p. 081101, 2007, https://doi.org/10.1063/1.2772756.

[4] L. Li, T. Li, S. Wang, S. Zhu, and X. Zhang, "Broad band focusing and demultiplexing of in-plane propagating surface plasmons," *Nano Lett.*, vol. 11, no. 10, pp. 4357–4361, 2011, https://doi.org/10.1021/nl2024855.

[5] L. Li, T. Li, S. M. Wang, and S. N. Zhu, "Collimated plasmon beam: nondiffracting versus linearly focused," *Phys. Rev. Lett.*, vol. 110, no. 4, p. 046807, 2013, https://doi.org/10.1103/PhysRevLett.110.046807.

[6] S. Dong, Y. Zhang, H. Guo, et al., "Highly efficient wave-front reshaping of surface waves with dielectric meta-walls," *Phys. Rev. Appl.*, vol. 9, no. 1, p. 014032, 2018, https://doi.org/10.1103/PhysRevApplied.9.014032.

[7] S. Dong, Z. Wang, H. Guo, et al., "Dielectric meta-walls for surface plasmon focusing and Bessel beam generation," *Europhys. Lett.*, vol. 122, no. 6, p. 67002, 2018, https://doi.org/10.1209/0295-5075/122/67002.

[8] W. Y. Tsai, Q. Sun, G. Hu, et al., "Twisted surface plasmons with spin-controlled gold surfaces," *Adv. Opt. Mater.*, vol. 7, no. 8, p. 1801060, 2019, https://doi.org/10.1002/adom.201801060.

[9] A. Drezet, D. Koller, A. Hohenau, A. Leitner, F. R. Aussenegg, and J. R. Krenn, "Plasmonic crystal demultiplexer and multiports," *Nano Lett.*, vol. 7, no. 6, pp. 1697–1700, 2007, https://doi.org/10.1021/nl070682p.

[10] A. Minovich, A. E. Klein, N. Janunts, T. Pertsch, D. N. Neshev, and Y. S. Kivshar, "Generation and near-field imaging of airy surface plasmons," *Phys. Rev. Lett.*, vol. 107, no. 11, p. 116802, 2011, https://doi.org/10.1103/physrevlett.107.116802.

[11] L. Li, T. Li, S. M. Wang, C. Zhang, and S. N. Zhu, "Plasmonic airy beam generated by in-plane diffraction," *Phys. Rev. Lett.*, vol. 107, no. 12, p. 126804, 2011, https://doi.org/10.1103/PhysRevLett.107.126804.

[12] P. A. Huidobro, M. L. Nesterov, L. Martín-Moreno, and F. J. García-Vidal, "Transformation optics for plasmonics," *Nano Lett.*, vol. 10, no. 6, pp. 1985–1990, 2010, https://doi.org/10.1021/nl100800c.

[13] J. S. Gomez-Diaz, M. Tymchenko, and A. Alù, "Hyperbolic plasmons and topological transitions over uniaxial metasurfaces," *Phys. Rev. Lett.*, vol. 114, no. 23, p. 233901, 2015, https://doi.org/10.1103/PhysRevLett.114.233901.

[14] G. Hu, A. Krasnok, Y. Mazor, C. W. Qiu, and A. Alù, *arXiv: 2001.03304 [Physics Optics]*, New York, Cornell University, 2020. (10 January 2020).

[15] Y. Liu, T. Zentgraf, G. Bartal, and X. Zhang, "Transformational plasmon optics," *Nano Lett.*, vol. 10, no. 6, pp. 1991–1997, 2010, https://doi.org/10.1021/nl1008019.

[16] H. Wei, Z. Li, X. Tian, et al., "Quantum dot-based local field imaging reveals plasmon-based interferometric logic in silver nanowire networks," *Nano Lett.*, vol. 11, no. 2, pp. 471–475, 2010, https://doi.org/10.1021/nl103228b.

[17] H. Wei, Z. Wang, X. Tian, M. Käll, and H. Xu, "Cascaded logic gates in nanophotonic plasmon networks," *Nat. Commun.*, vol. 2, no. 1, p. 387, 2011, https://doi.org/10.1038/ncomms1388.

[18] Y. Fang, Z. Li, Y. Huang, et al., "Branched silver nanowires as controllable plasmon routers," *Nano Lett.*, vol. 10, no. 5, pp. 1950–1954, 2010, https://doi.org/10.1021/nl101168u.

[19] H. Wei, D. Pan, and H. Xu, "Routing of surface plasmons in silver nanowire networks controlled by polarization and coating," *Nanoscale*, vol. 7, no. 45, pp. 19053–19059, 2015, https://doi.org/10.1039/C5NR02511G.

[20] S. Kim, S. Bailey, M. Liu, and R. Yan, "Decoupling co-existing surface plasmon polariton (SPP) modes in a nanowire plasmonic waveguide for quantitative mode analysis," *Nano Res.*, vol. 10, no. 7, pp. 2395–2404, 2017, https://doi.org/10.1007/s12274-017-1438-1.

[21] R. F. Oulton, V. J. Sorger, D. A. Genov, D. F. Pile, and X. Zhang, "A hybrid plasmonic waveguide for sub-wavelength confinement and long-range propagation," *Nat. Photonics*, vol. 2, no. 8, pp. 496–500, 2008, https://doi.org/10.1038/nphoton.2008.131.

[22] D. Ansell, I. P. Radko, Z. Han, F. J. Rodriguez, S. I. Bozhevolnyi, and A. N. Grigorenko, "Hybrid graphene plasmonic waveguide modulators," *Nat. Commun.*, vol. 6, no. 1, p. 8846, 2015, https://doi.org/10.1038/ncomms9846.

[23] H. Siampour, S. Kumar, V. A. Davydov, L. F. Kulikova, V. N. Agafonov, and S. I. Bozhevolnyi, "On-chip excitation of single germanium vacancies in nanodiamonds embedded in plasmonic waveguides," *Light Sci. Appl.*, vol. 7, no. 1, pp. 1–9, 2018, https://doi.org/10.1038/s41377-018-0062-5.

[24] H. Siampour, S. Kumar, and S. I. Bozhevolnyi, "Nanofabrication of plasmonic circuits containing single photon sources," *ACS Photonics*, vol. 4, no. 8, pp. 1879–1884, 2017, https://doi.org/10.1021/acsphotonics.7b00374.

[25] H. Siampour, S. Kumar, and S. I. Bozhevolnyi, "Chip-integrated plasmonic cavity-enhanced single nitrogen-vacancy center emission," *Nanoscale*, vol. 9, no. 45, pp. 17902–17908, 2017, https://doi.org/10.1039/C7NR05675C.

[26] M. Ono, M. Hata, M. Tsunekawa, et al., "Ultrafast and energy-efficient all-optical switching with graphene-loaded deep-subwavelength plasmonic waveguides," *Nat. Photonics*, vol. 14, no. 1, pp. 37–43, 2020, https://doi.org/10.1038/s41566-019-0547-7.

[27] S. I. Bozhevolnyi, V. S. Volkov, E. Devaux, J. Y. Laluet, and T. W. Ebbesen, "Channel plasmon subwavelength waveguide components including interferometers and ring resonators," *Nature*, vol. 440, no. 7083, pp. 508–511, 2006, https://doi.org/10.1038/nature04594.

[28] N. Yu, P. Genevet, M. A. Kats, et al., "Light propagation with phase discontinuities: generalized laws of reflection and refraction," *Science*, vol. 334, no. 6054, pp. 333–337, 2011, https://doi.org/10.1126/science.1210713.

[29] S. Sun, Q. He, S. Xiao, Q. Xu, X. Li, and L. Zhou, "Gradient-index meta-surfaces as a bridge linking propagating waves and surface waves," *Nat. Mater.*, vol. 11, no. 5, pp. 426–431, 2012, https://doi.org/10.1038/nmat3292.

[30] X. Yin, Z. Ye, J. Rho, Y. Wang, and X. Zhang, "Photonic spin Hall effect at metasurfaces," *Science*, vol. 339, no. 6126, pp. 1405–1407, 2013, https://doi.org/10.1126/science.1231758.

[31] W. Luo, S. Xiao, Q. He, S. Sun, and L. Zhou, "Photonic spin Hall effect with nearly 100% efficiency," *Adv. Opt. Mater.*, vol. 3, no. 8, pp. 1102–1108, 2015, https://doi.org/10.1002/adom.201500068.

[32] G. Hu, X. Hong, K. Wang, et al., "Coherent steering of nonlinear chiral valley photons with a synthetic Au–WS2 metasurface," *Nat. Photonics*, vol. 13, no. 7, pp. 467–472, 2019, https://doi.org/10.1038/s41566-019-0399-1.

[33] L. Huang, X. Chen, H. Mühlenbernd, et al., "Three-dimensional optical holography using a plasmonic metasurface," *Nat. Commun.*, vol. 4, no. 1, p. 2808, 2013, https://doi.org/10.1038/ncomms3808.

[34] G. Zheng, H. Mühlenbernd, M. Kenney, G. Li, T. Zentgraf, and G. Zhang, "Metasurface holograms reaching 80% efficiency," *Nat. Nanotechnol.*, vol. 10, no. 4, pp. 308–312, 2015, https://doi.org/10.1038/nnano.2015.2.

[35] W. T. Chen, K. Y. Yang, C. M. Wang, et al., "High-efficiency broadband meta-hologram with polarization-controlled dual images," *Nano Lett.*, vol. 14, no. 1, pp. 225–230, 2014, https://doi.org/10.1021/nl403811d.

[36] K. Chen, G. Ding, G. Hu, et al., "Directional janus metasurface," *Adv. Mater.*, vol. 32 no. 2, p. 1906352, 2019, https://doi.org/10.1002/adma.201906352.

[37] J. Zhou, H. Qian, G. Hu, H. Luo, S. Wen, and Z. Liu, "Broadband photonic spin Hall meta-lens," *ACS Nano*, vol. 12, no. 1, pp. 82–88, 2017, https://doi.org/10.1021/acsnano.7b07379.

[38] A. Arbabi, Y. Horie, A. J. Ball, M. Bagheri, and A. Faraon, "Subwavelength-thick lenses with high numerical apertures and large efficiency based on high-contrast transmit arrays," *Nat. Commun.*, vol. 6, no. 1, pp. 1–6, 2015, https://doi.org/10.1038/ncomms8069.

[39] M. Khorasaninejad, W. T. Chen, R. C. Devlin, et al., "Metalenses at visible wavelengths: Diffraction-limited focusing and subwavelength resolution imaging," *Science*, vol. 352, no. 6290, pp. 1190–1194, 2016, https://doi.org/10.1126/science.aaf6644.

[40] A. Pors, M. G. Nielsen, T. Bernardin, J. C. Weeber, and S. I. Bozhevolnyi, "Efficient unidirectional polarization-controlled

excitation of surface plasmon polaritons," *Light Sci. Appl.*, vol. 3, no. 8, p. e197, 2014, https://doi.org/10.1038/lsa.2014.78.

[41] H. Mühlenbernd, P. Georgi, N. Pholchai, et al., "Amplitude-and phase-controlled surface plasmon polariton excitation with metasurfaces," *ACS Photonics*, vol. 3, no. 1, pp. 124–129, 2016, https://doi.org/10.1021/acsphotonics.5b00536.

[42] W. Sun, Q. He, S. Sun, and L. Zhou, "High-efficiency surface plasmon meta-couplers: concept and microwave-regime realizations," *Light Sci. Appl.*, vol. 5, no. 1, p. e16003, 2016, https://doi.org/10.1038/lsa.2016.3.

[43] J. Kischkat, S. Peters, B. Gruska, et al., "Mid-infrared optical properties of thin films of aluminum oxide, titanium dioxide, silicon dioxide, aluminum nitride, and silicon nitride," *Appl. Opt.*, vol. 51, no. 28, pp. 6789–6798, 2012, https://doi.org/10.1364/AO.51.006789.

Supplementary Material: The online version of this article offers supplementary material (https://doi.org/10.1515/nanoph-2020-0078).